Thiol-Retaining N-Terminal Cysteine Chemistry for Dual Modification and Bicyclic Peptide Construction

Junjie Liu[1], Shixiang Duan[1], Yang Huang[2], Chuanliu Wu[3,*], Yi-Lin Wu[4,*], and Yu-Hsuan Tsai[1,*]

[1] Institute of Molecular Physiology, Shenzhen Bay Laboratory, Shenzhen 518132, China

[2] Key Laboratory of Biocatalysis & Chiral Drug Synthesis of Guizhou Province, Generic Drug Research Center of Guizhou Province, School of Pharmacy, Zunyi Medical University, Zunyi 563000, China

[3] Department of Chemistry, College of Chemistry and Chemical Engineering, The MOE Key Laboratory of Spectrochemical Analysis and Instrumentation, State Key Laboratory of Physical Chemistry of Solid Surfaces, Xiamen University, Xiamen 361005, China

[4] Department of Applied Chemistry, National Yang Ming Chiao Tung University, Hsinchu 30010, Taiwan

* Correspondence: chlwu@xmu.edu.cn; yilin.wu@nycu.edu.tw; tsai.y-h@outlook.com

Abstract

N-terminal cysteine presents a uniquely reactive 1,2-aminothiol motif that enables site-specific modification of peptides and proteins composed solely of canonical amino acids. For both in vitro and in vivo applications, this operationally simple chemistry is an attractive alternative to bioorthogonal strategies that require noncanonical handles. However, most 1,2-aminothiol-selective reagents irreversibly consume both the amine and thiol, yielding inert heterocycles and limiting downstream diversification. Here we report a thiol-retaining N-terminal cysteine chemistry by repurposing 2-((alkyl**t**hio)(**a**ryl/alkyl)**m**ethylene)**m**alononitriles (TAMMs) to favor a thiol-containing conjugate over the canonical cyclized product. Through rational design and mechanistic analysis of *ortho*-substituted TAMMs (*o*-TAMMs), we establish steric hindrance as a key determinant of thiol-retaining adduct stability. The retained thiol provides an immediate handle for sequential dual modification of peptides and proteins. Extending this concept to scaffold design, an electrophile-equipped *o*-TAMM crosslinker converts CX_mCX_nC peptides into compact bicyclic architectures comprising a thioether ring and a disulfide ring. Phage display using this chemistry affords high-affinity bicyclic binders of KEAP1, and the disulfide can be transformed into a redox-stable thioacetal without loss of affinity. Collectively, this work establishes a mechanistically grounded platform for thiol-retaining N-terminal cysteine ligation, enabling dual functionalization and access to structurally distinctive bicyclic peptides.

Main Text

Precise chemical modification of peptides and proteins underpins applications ranging from mechanistic biology to diagnostics and therapeutics.[1-7] Many established bioorthogonal reactions rely on noncanonical functionalities introduced via enzymatic tagging or engineered translation systems, which can be costly and suffer from reduced protein yields.[7-10] In contrast, strategies that directly target canonical amino acids are operationally simple and readily deployed across diverse biological settings.[11] In this context, N-terminal cysteine is a privileged handle.[12] Its 1,2-aminothiol motif is distinctive in native proteomes because protein translation initiates from methionine,

enabling high chemoselectivity with minimal background interference.

Such a feature has inspired the development of reagents that preferentially engage N-terminal cysteine, including 2-cyanobenzothiazole (CBT),[13] 2-formylphenyl boronic acid,[14] 2-benzylacrylaldehyde,[15] cyclopropenone,[16] and NHS-activated acrylamide.[17] Despite their structural diversity, these reagents share a common mechanistic outcome: tandem nucleophilic additions of the thiol and amine that irreversibly consume both functionalities to form chemically inert heterocycles. As a result, ligation at N-terminal cysteine typically precludes further derivatization, limiting modular diversification and access to higher-order architectures.[12]

Native chemical ligation represents a notable exception, as it can furnish thiol-containing products.[18] However, the instability of thioester substrates, the reliance on thiol additives, slow kinetics (ca. 0.1 M^{-1} s^{-1}), and frequently denaturing conditions restrict its direct use for modifying proteins on living cell surfaces.[19] Consequently, a general and rapid 1,2-aminothiol ligation that preserves thiol functionality remains a long-standing unmet need.

We recently reported a mechanistic analysis of the reaction between 2-((alkyl**t**hio)(**a**ryl)**m**ethylene)**m**alononitriles (TAMMs, **1**; **Fig. 1a**) and 1,2-aminothiols (**2**), revealing a *kinetically accessible* thiol-containing enamine intermediate (**5**).[20] Stabilizing this intermediate would represent a significant conceptual advance; it would retain the nucleophilic thiol at the N-terminus, enabling direct derivatization and compact crosslinking (**Fig. 1b**). In particular, pairing the TAMM-derived linkage with the liberated thiol near the N-terminus offers a route to tight bicyclic topologies (thioether plus disulfide rings) from CX_mCX_nC peptides (**Fig. 1c**). Such compact architectures can reduce conformational entropy and increase scaffold rigidity, features that are advantageous for discovering high-affinity peptide binders.[21-23]

A key limitation, however, is that enamine **5** is typically short-lived, rapidly converting into the thermodynamically favored dihydrothiazole **6**, which irreversibly consumes the thiol and prevents practical exploitation of this intermediate. We reasoned that this outcome is not inevitable but rather reflects conformational and kinetic preferences embedded in the TAMM scaffold. Here we show that steric hindrance can be leveraged as a reagent-level design principle to reshape the reaction landscape. By introducing steric congestion at the β-position of TAMMs, we suppress thiol-consuming cyclization pathways and stabilize thiol-retaining enamine adducts, enabling their isolation and downstream functionalization.

Mechanistically, TAMM **1** first undergoes thiol exchange with 1,2-aminothiol **2** to form **3** (step *a*), which rapidly cyclizes to thiazolidine **4** (step *b*). Conversion of **4** to **5** (step *c*) is kinetically favored but reversible, while formation of the thermodynamically more stable **6** (step *d*) is slower yet effectively irreversible. Consequently, **5** ultimately becomes **6**. Consistent with step *c* being faster than step *d*, accelerating step *a* increases the extent of **5** accumulation, although only transiently.[20] Inspired by prior work showing that steric hindrance adjacent to a 1,2-aminothiol can affect the lifetime of a CBT condensation intermediate,[24] we set out to evaluate whether increasing congestion on the TAMM scaffold could stabilize thiol-retaining adduct **5**.

Consistent with this idea, reaction of *ortho*-methylphenyl TAMM **1a** and peptide **2x** (H-CGGKGW-OH) in 0.1 M $NaHCO3_{(aq)}$ produced thiol-containing enamine **5ax** as the sole detectable product (**Fig. 1a**). Its identity was supported by alkylation with iodoacetamide (**Fig. S3**). Notably, **5ax** remained stable upon overnight incubation, with no detectable formation of **6ax** (**Fig. S4**). We then synthesized a series of *ortho*-substituted TAMMs (*o*-TAMMs) **1b**-**1i** and evaluated their reactions with **2x** (**Fig. 1** and **S5**-**S12**). Bulky substituents (**1c**-**1g**) consistently favored formation of **5** (**Figs. S6**-**S10**). Intriguingly, **1b** ($R^4 = CF_3$) showed only partial conversion (**Fig. S5**), while *o*-TAMMs **1h** and **1i** with small substituents gave dihydrothiazole **6** as the exclusive product (**Figs. S11** and **S12**). We further examined two alkyl TAMMs **1j** and **1k**, derived from pivalic acid and 3,3-dimethylbutanoic acid, respectively. TAMM **1j** yielded only **6jx** (**Fig. S13**), whereas **1k** produced a mixture of **5kx** and **6kx** after overnight incubation (**Fig. S14**).

Collectively, these data indicate β-substitution as a key determinant of product selectivity. Bulky β-substituents likely suppress the reverse conversion of **5** to **4** and/or slow the subsequent formation of **6**, enabling isolation of **5** as a stable thiol-retaining product.

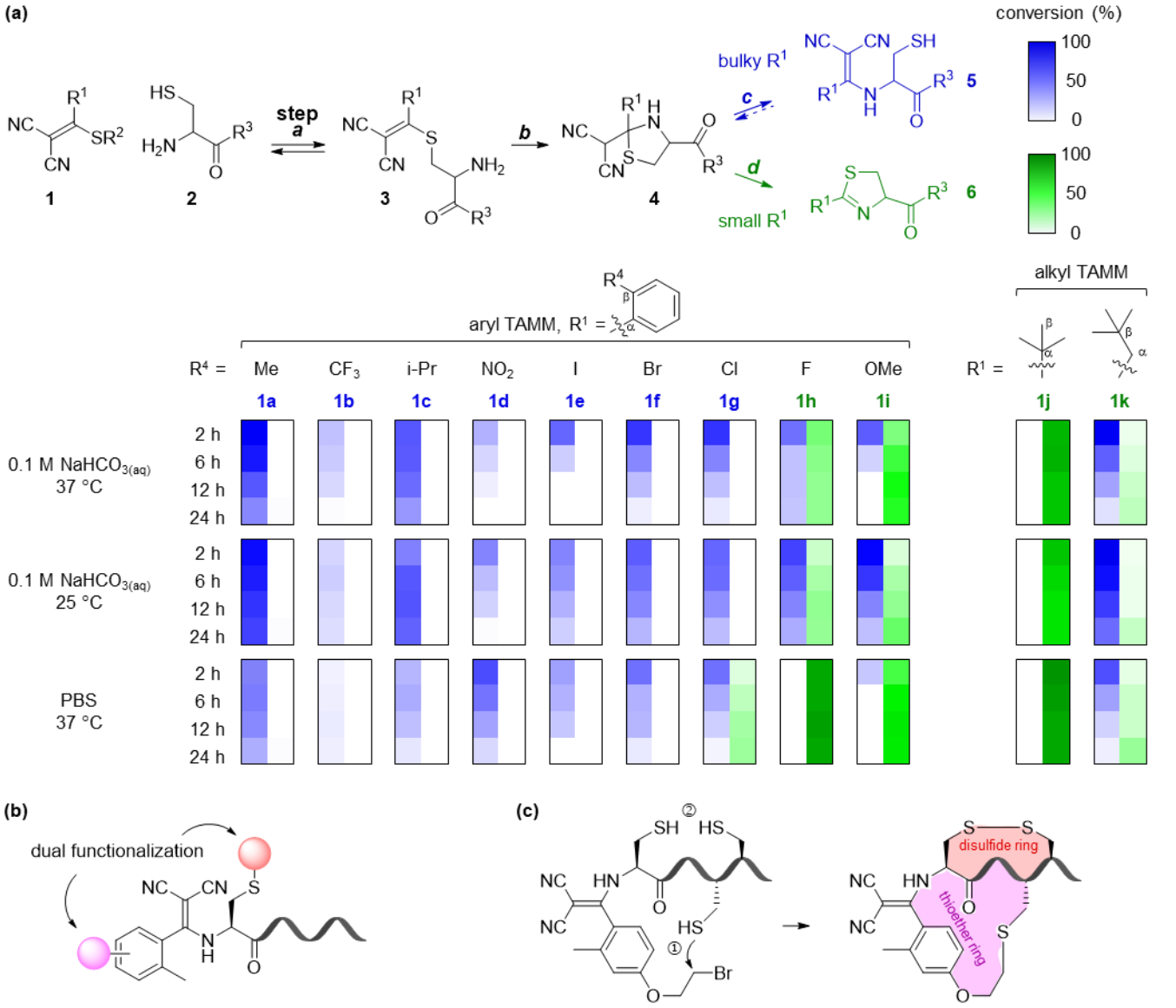

Figure 1. Thiol-retaining N-terminal cysteine modification enabled by steric regulation (a), with applications in dual functionalization (b) and construction of compact bicyclic topologies (c). Conversions were quantified by HPLC for reactions of peptide 50 μM **2x** and 200 μM **1** in the presence of 500 μM TCEP and 500 μM Ac-Cys-OMe under the indicated conditions.

Bulky *o*-TAMMs also display more complex ^{1}H NMR behavior, consistent with restricted conformational dynamics. At 25 °C in $CDCl_3$, *o*-TAMMs **1a**-**1g** display a doublet-like resonance for the methyl ester protons, whereas these protons appear as a singlet in **1h**-**1k** (see **Supporting Information**). Particularly, in DMSO-d_6, several resonances of **1a** appear as two sets of peaks (ca. 55:45) at 25 °C but coalesce at 75 °C (**Figs. 2a** and **S15a**). Similar behavior was observed for *ortho*-iodo substituted **1e** (**Fig. S15b**), as well as *ortho*-nitro substituted **1d** (**Fig. S16a**) and **1l** (R^2 = CH_2CF_3, **Fig. S16b**). By contrast, *o*-TAMMs bearing small substituents (e.g., R^4 = F for **1h** or OMe for **1i**) show peak splitting only at low temperature (**Figs. 2b**, **S17** and **S18**). This behavior parallels that of enamine **5**, where conjugation between the nitrogen lone pair and the dicyanovinyl acceptor increases C–N bond order and slows rotation.

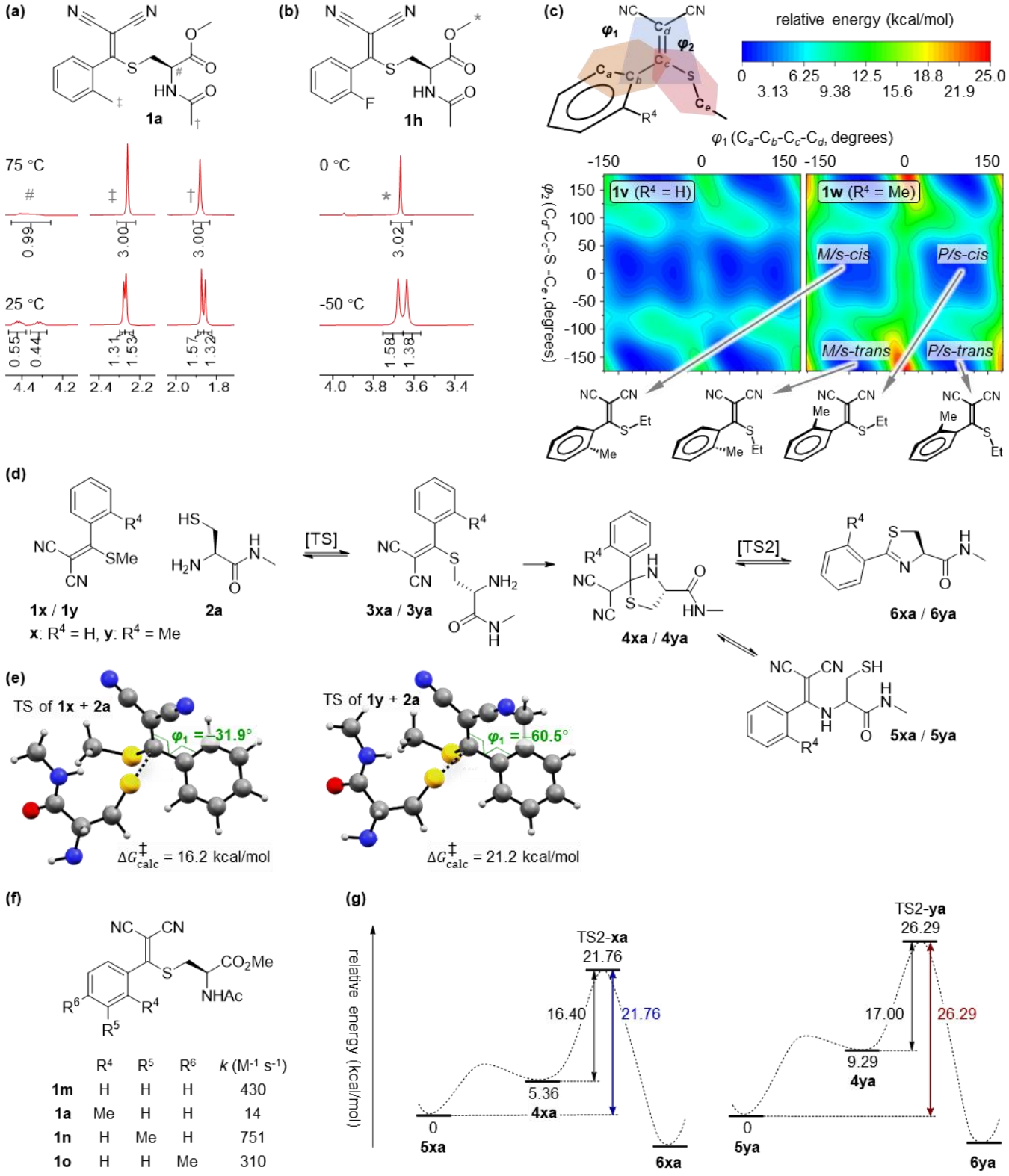

Figure 2. Mechanistic investigation of *o*-TAMM. (a,b) Variable-temperature ^{1}H NMR spectra, showcasing different rotational barriers of **1a** and **1h**. See **Figs. S15** and **S17** for the full spectra. (c) Calculated energy profiles of **1v** (R^2 = Et, R^4 = H) and **1w** (R^2 = Et, R^4 = Me), confirming that a bulky *ortho* substituent increases the conformational interconversion barrier. (d) Model thiolate-exchange reactions of **1x** (R^2 = Me, R^4 = H) or **1y** (R^2 = R^4 = Me) with **2a** used for DFT calculations of transition states and reaction barriers. (e) Ortho-methyl substitution increases the activation barrier for thiolate exchange, consistent with reduced aryl–dicyanovinyl conjugation in the transition state (TS). (f) Experimentally measured consumption rate constants of representative TAMMs in Tris buffer (pH 8.5) at 37 °C. (g) Relative energies of **4**-**6** and TS2 rationalize stabilization of *ortho*-methyl substituted **5** at room temperature, by increasing the effective barrier for conversion to **4** and suppressing formation of **6**.

Computational analysis[25] further supports a steric origin for these effects. Conformational scans of model compounds **1v** (R^2 = Et, R^4 = H) and **1w** (R^2 = Et, R^4 = Me) reveal low-energy clusters corresponding to P/M atropisomers and *s-cis*/*s-trans* forms (**Fig. 2c**). Steric hindrance increases the barrier for *P*/*s-cis* ⇌ *M*/*s-cis* interconversion from 3.9 kcal/mol for **1v** to 9.7 kcal/mol for **1w**, consistent with the distinct conformer populations observed by ^{1}H NMR. Steric congestion also impacts reactivity. DFT calculations[26-27] on thiolate exchange between cysteine methyl amide (Cys-NHMe, **2a**) and TAMM **1x** (R^2 = Me, R^4 = H) or **1y** (R^2 = R^4 = Me) indicate a higher activation free energy (21.2 vs 16.2 kcal/mol) for the sterically congested system (**Fig. 2d**). The increase correlates with a larger aryl–dicyanovinyl dihedral angle (60.5° vs 31.9°; **Fig. 2e**), which weakens π-conjugative stabilization in the transition state (TS). Experimentally, **2x** reacts more slowly with *o*-TAMM **1a** than unsubstituted, *meta*- or *para*-substituted TAMMs (**Fig.2f** and **S19**). Finally, steric congestion raises the effective barrier for malononitrile elimination. While the intrinsic elimination barrier (TS2) is similar for R^4 = H (16.4 kcal/mol) and R^4 = Me (17.0 kcal/mol; **Figs. 2g** and **S20**), *ortho*-methyl substitution substantially increases the energy gap between **5** and **4** from 5.4 kcal/mol to 9.3 kcal/mol. Consequently, the effective barrier for elimination increases from 21.8 kcal/mol to 26.3 kcal/mol (see **Supporting Information** for discussion), shifting the reaction outcome toward **5**. Consistent with a higher barrier, heating **5ax** to 90 °C could yield some **6ax** (**Fig. S21**). Together, these data explain how steric hindrance stabilizes enamine **5** and suppresses dihydrothiazole formation at room temperature.

We next evaluated *o*-TAMMs for site-specific modification of peptides and proteins. *O*rtho-methyl TAMMs **1a** and **1p** were reacted with peptides **2x** (H-CGGKGW-OH) and **2y** (H-CPVRYGWDMRC-OH), as well as zHER2 and SUMO proteins engineered with an N-terminal cysteine (**Fig. 3a**). In each case, high conversion to the thiol-retaining enamine products was observed. TAMM **1p** further incorporates a *para*-homopropargyl group, enabling modular installation of diverse functionalities using commercially available azides through Cu-catalyzed azide-alkyne cycloaddition (CuAAC). As a proof of concept, peptide conjugate **5px** (from **1p** and **2x**) underwent sequential derivatization: maleimide capping of the liberated thiol afforded **7px**, followed by CuAAC with 2-azidoethanol to yield dual-functionalized **8px** (**Figs. 3b** and **S22**). The same strategy was validated on peptide **2y**, which contains two cysteines, where both thiols were efficiently modified by maleimide (**Figs. 3b** and **S23**). Together, these results establish *o*-TAMMs as a general platform for thiol-retaining N-terminal cysteine ligation and dual modification.

The thiol retained in enamine **5** can also engage an internal cysteine to form a disulfide bond, yielding side-chain-cyclized peptides. In parallel, TAMM reagents can be equipped with thiol-reactive handles to enable thioether-based cyclization.[28-30] Combining these concepts, we designed *o*-TAMM **1q**, featuring an *ortho*-methyl group to stabilize enamine **5** and a *para*-substituted alkyl bromide as a thiol-reactive electrophile. We envisaged that reaction of **1q** and CX_mCX_nC sequences would yield bicyclic scaffolds containing both a disulfide ring and a thioether ring (**Fig. 4a**). A key requirement is chemoselectivity: the alkyl bromide must react with an internal cysteine rather than the N-terminal thiol generated upon enamine formation.

We therefore tested **1q** with peptides containing an N-terminal cysteine and 0, 1, or 2 internal cysteines (i.e., **2x**, **2y**, or **2z**). With **2x**, **1q** produced the expected enamine **5qx** (**Fig. S24**). With **2y**, we observed formation of a cyclized adduct consistent with intramolecular substitution and HBr loss to form a thioether linkage (**Fig. S25**). These results indicate that the alkyl bromide in **1q** preferentially undergoes substitution with an internal cysteine while sparing the N-terminal thiol. Reaction of **1q** with **2z** afforded two peaks of identical mass (**Fig. S26**), assigned to alternative monocyclic peptide (**MCP**) products formed by thioether cyclization through either Cys10 or Cys15 (**Fig. 4a**). Subsequent oxidation afforded two well-resolved bicyclic peptide (**BCP**) isomers by HPLC.

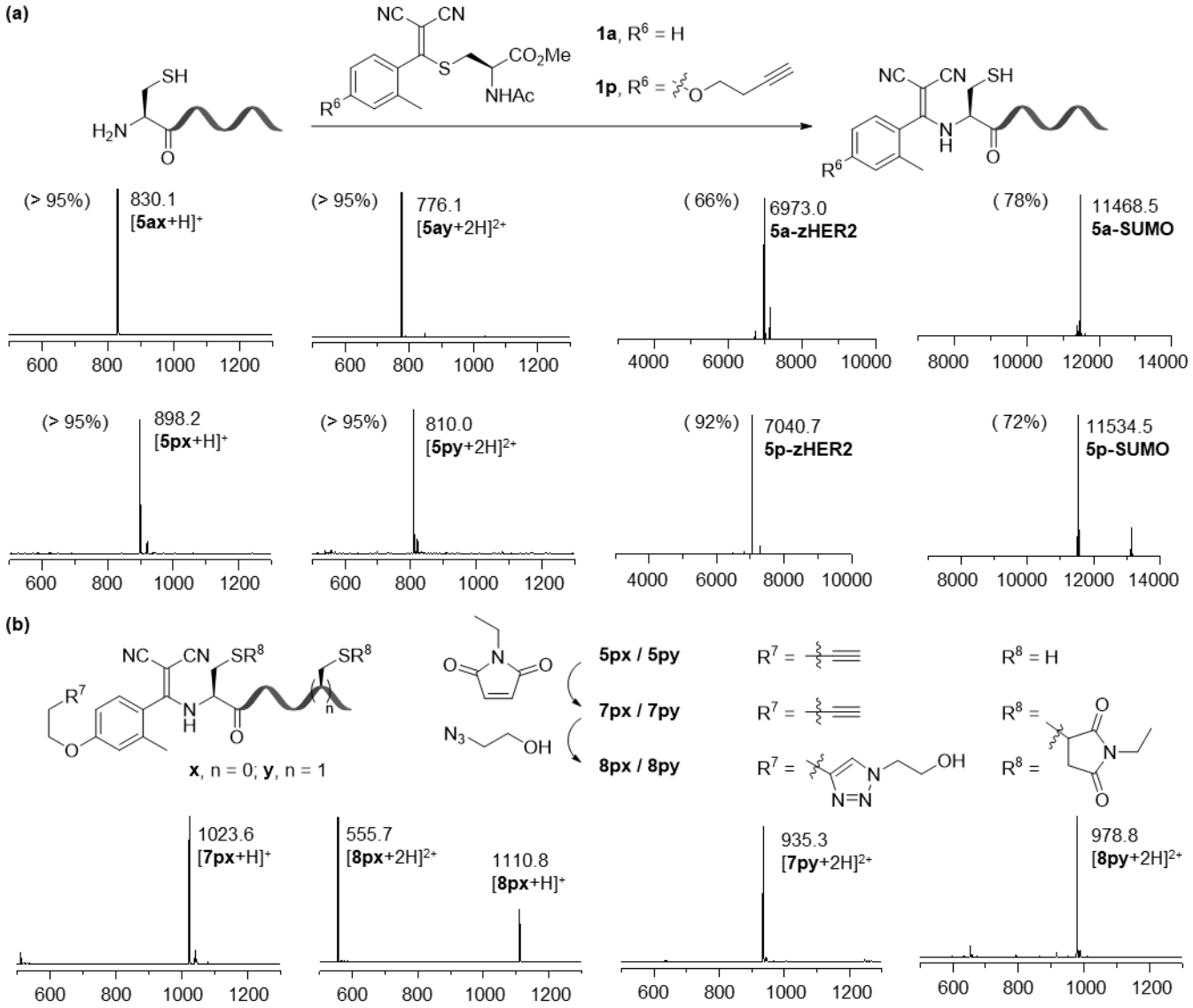

Figure 3. Site-specific functionalization of peptides and proteins via thiol-retaining N-terminal cysteine chemistry. (a) Reaction of TAMM **1a** or alkyne-bearing TAMM **1p** with the N-terminal cysteine of peptides **2x** and **2y**, as well as proteins zHER2 and SUMO, to afford the corresponding thiol-retaining enamine conjugates (**5a** or **5p** derivatives). (b) Sequential diversification of **5px** or **5py** by thiol conjugation with ethyl maleimide, followed by CuAAC with 2-azidoethanol for dual functionalization.

With the reactivity and selectivity established, we applied **1q** to construct a phage-displayed bicyclic peptide library and selected binders to KEAP1 (**Fig. 4b**). The phages exhibited substantial enrichment over three rounds (~0.2-fold, ~590-fold, and ~1600-fold enrichment; **Fig. 4c**, **4d** and **S27**). Next-generation sequencing identified conserved, recurring sequences among top hits (**Fig. S28**). We selected sequence A3-4 (CTGWEPETGECRETQC), the most abundant after rounds 1 and 2, for characterization. Two bicyclic isomers, **BCP-a** and **BCP-b**, were synthesized and showed dissociation constants of 312 nM and 108 nM for KEAP1 by surface plasmon resonance (SPR) (**Figs. S29**). In contrast, the linear analogue (**LP**) with all cysteines mutated to alanines displayed negligible affinity (K_D = 4160 nM, **Fig. S29**). Moreover, the disulfide in **BCP-a** could be converted to a redox-stable thioacetal (**BCP-a'**) through reaction with methylene iodide without loss of KEAP1 affinity. These results demonstrate that *o*-TAMM enabled bicyclization supports discovery of high-affinity bicyclic binders with a compact topology and a tunable redox element.

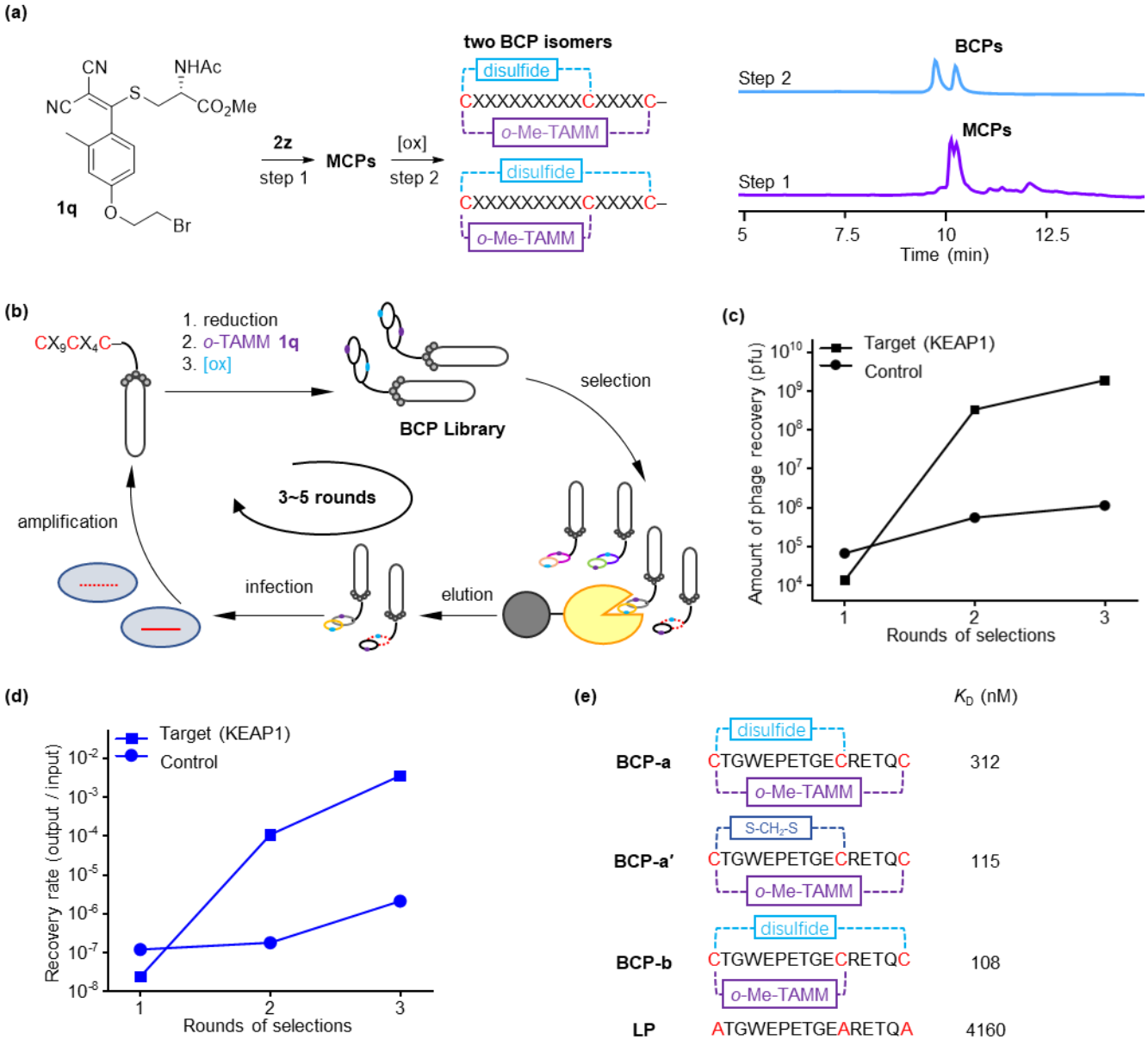

Figure 4. TAMM-mediated peptide cyclization and phage display discovery of bicyclic peptide binders. (a) Construction of bicyclic peptides from *o*-TAMM crosslinker **1q** and peptide **2z** (H-CGGRGGRGGSCGGRGCGW-NH_2). Initial thioether cyclization affords two monocyclic peptide (**MCP**) regioisomers, which are resolved by chromatography; subsequent oxidation yields the corresponding bicyclic peptide (**BCP**) isomers. (b) Scheme for the phage display of a CX_9CX_4C sequence at the N-terminal of g3p proteins for screening cyclic peptide binders against KEAP1. (c) Recovery amount and (d) efficiency (output/input phage ratio) of phages after iterative selection against target protein KEAP1 (squares) and negative control (circles). Concurrent increases in recovery amount and efficiency reflect the enrichment of specific binders. (e) KEAP1 binding affinities of A3-4 bicyclic isoforms measured by SPR. Representative sensorgrams are shown in **Fig. S29**.

In summary, this work introduces a steric-control strategy that shifts the chemistry of TAMM and 1,2-aminothiol from thiol-consuming cyclization to thiol-retaining ligation. The key advance is a reagent-level design that stabilizes a normally transient thiol-containing intermediate. Computational analysis indicates that steric congestion suppresses reversal of step *c*, making the thiol-retaining adduct persistent and usable for subsequent transformations. This platform offers at least two complementary capabilities. First, it enables dual modification of N-terminal cysteine peptides and proteins by combining the retained thiol with functionality carried by the TAMM reagent or an added orthogonal handle. Second, it enables compact bicyclic peptide construction through chemoselective reaction of internal cysteines using an electrophile-equipped *o*-TAMM. By linking mechanistic

understanding to reagent design and functional applications, this chemistry expands the synthetic scope of N-terminal cysteine modification and provides a practical route to structurally distinctive bicyclic peptide ligands.

Acknowledgements

We are grateful to Shenzhen Bay Laboratory (SZBL) and the National Natural Science Foundation of China (22277079 to YHT) for financial support. We thank the SZBL Biomedical Research Core Facilities and the SMART Bio-Tech Center for technical assistance.

References

(1) Huang, Y.; Zhang, P.; Wang, H.; Chen, Y.; Liu, T.; Luo, X. Genetic Code Expansion: Recent Developments and Emerging Applications. *Chem. Rev.* **2025,** *125* (2), 523–598.
(2) Li, J. P.; Guo, W.; Zou, P.; Chu, C.; Wu, J.; Guo, Z.; Huang, Y.; Yang, J.; Chen, P. R. Molecular tools for decoding multicellular systems: from mechanisms to medicine. *Natl. Sci. Rev.* **2025,** *12* (12), nwaf473.
(3) Liu, S.; Hua, C.; Li, X.; Yuan, P.; Xing, B. A powerful bioorthogonal toolbox boosting the development of immune theranostics. *Chem. Sci.* **2025,** *16* (48), 22870–22899.
(4) Moller, D. N.; Kofoed, C.; Thygesen, M. B.; Jensen, K. J. Peptide Tags for Site-Selective Nonenzymatic Covalent Modification of Proteins. *J. Pept. Sci.* **2025,** *31* (11), e70058.
(5) Mitry, M. M. A.; Greco, F.; Osborn, H. M. I. In Vivo Applications of Bioorthogonal Reactions: Chemistry and Targeting Mechanisms. *Chem. Eur. J.* **2023,** *29* (20), e202203942.
(6) Scinto, S. L.; Bilodeau, D. A.; Hincapie, R.; Lee, W.; Nguyen, S. S.; Xu, M.; Am Ende, C. W.; Finn, M. G.; Lang, K.; Lin, Q.; Pezacki, J. P.; Prescher, J. A.; Robillard, M. S.; Fox, J. M. Bioorthogonal chemistry. *Nat. Rev. Methods Primers* **2021,** *1*, 30.
(7) Hayes, H. C.; Luk, L. Y. P.; Tsai, Y.-H. Approaches for peptide and protein cyclisation. *Org. Biomol. Chem.* **2021,** *19* (18), 3983–4001.
(8) Dunkelmann, D. L.; Chin, J. W. Engineering Pyrrolysine Systems for Genetic Code Expansion and Reprogramming. *Chem. Rev.* **2024,** *124* (19), 11008–11062.
(9) Chen, J. H.; Tsai, Y.-H. Applications of genetic code expansion in studying protein post-translational modification. *J. Mol. Biol.* **2022,** *434* (8), 167424.
(10) Nödling, A. R.; Spear, L. A.; Williams, T. L.; Luk, L. Y. P.; Tsai, Y.-H. Using genetically incorporated unnatural amino acids to control protein functions in mammalian cells. *Essays Biochem.* **2019,** *63* (2), 237–266.
(11) Kim, Y.; Yi, H. B.; Seo, K.; Lee, H. S.; Shin, I. Site-selective modification of native proteins. *Trends in Chemistry* **2025,** *7* (5), 240–254.
(12) Chen, F. J.; Gao, J. M. Fast cysteine bioconjugation chemistry. *Chem. Eur. J.* **2022,** *28* (66), e202201843.
(13) Ren, H.; Xiao, F.; Zhan, K.; Kim, Y. P.; Xie, H.; Xia, Z.; Rao, J. A biocompatible condensation reaction for the labeling of terminal cysteine residues on proteins. *Angew. Chem. Int. Ed.* **2009,** *48* (51), 9658–9662.
(14) Cambray, S.; Gao, J. Versatile Bioconjugation Chemistries of ortho-Boronyl Aryl Ketones and Aldehydes. *Acc. Chem. Res.* **2018,** *51* (9), 2198–2206.
(15) Wu, Y. Q.; Li, C.; Fan, S. H.; Zhao, Y. B.; Wu, C. L. Fast and Selective Reaction of 2-Benzylacrylaldehyde with 1,2-Aminothiol for Stable N-Terminal Cysteine Modification and Peptide Cyclization. *Bioconj. Chem.* **2021,** *32* (9), 2065–2072.
(16) Istrate, A.; Geeson, M. B.; Navo, C. D.; Sousa, B. B.; Marques, M. C.; Taylor, R. J.; Journeaux, T.; Oehler, S. R.; Mortensen, M. R.; Deery, M. J.; Bond, A. D.; Corzana, F.; Jiménez-Osés, G.; Bernardes, G. J. L. Platform for Orthogonal N-Cysteine-Specific Protein Modification Enabled by Cyclopropenone Reagents. *J. Am. Chem. Soc.* **2022,** *144* (23), 10396–10406.
(17) Silva, M. J. S. A.; Faustino, H.; Coelho, J. A. S.; Pinto, M. V.; Fernandes, A.; Compañón, I.; Corzana, F.; Gasser, G.;

Gois, P. M. P. Efficient Amino-Sulfhydryl Stapling on Peptides and Proteins Using Bifunctional NHS-Activated Acrylamides. *Angew Chem Int Edit* **2021,** *60* (19), 10850–10857.

(18) Conibear, A. C.; Watson, E. E.; Payne, R. J.; Becker, C. F. W. Native chemical ligation in protein synthesis and semi-synthesis. *Chem. Soc. Rev.* **2018,** *47* (24), 9046–9068.

(19) Gavins, G. C.; Gröger, K.; Bartoschek, M. D.; Wolf, P.; Beck-Sickinger, A. G.; Bultmann, S.; Seitz, O. Live cell PNA labelling enables erasable fluorescence imaging of membrane proteins. *Nat. Chem.* **2021,** *13* (1), 15–23.

(20) Huang, Y.; Wu, C.; Lu, A.; Wang, J.; Liang, J.; Sun, H.; Yang, L.; Duan, S.; Berezin, A. A.; Wu, C.; Zhang, B.; Wu, Y.-L.; Tsai, Y.-H. A Single Bioorthogonal Reaction for Multiplex Cell Surface Protein Labeling. *J. Am. Chem. Soc.* **2025,** *147* (2), 1612–1623.

(21) Rhodes, C. A.; Pei, D. Bicyclic peptides as next-generation therapeutics. *Chem. Eur. J.* **2017,** *23* (52), 12690–12703.

(22) Bozovicar, K.; Bratkovic, T. Small and Simple, yet Sturdy: Conformationally Constrained Peptides with Remarkable Properties. *Int. J. Mol. Sci.* **2021,** *22* (4), 1611.

(23) Chen, F. J.; Pinnette, N.; Gao, J. Strategies for the Construction of Multicyclic Phage Display Libraries. *ChemBioChem* **2024,** *25* (9), e202400072.

(24) Wang, W.; Gao, J. N, S-Double Labeling of N-Terminal Cysteines via an Alternative Conjugation Pathway with 2-Cyanobenzothiazole. *J. Org. Chem.* **2020,** *85* (3), 1756–1763.

(25) Bannwarth, C.; Ehlert, S.; Grimme, S. GFN2-xTB—An Accurate and Broadly Parametrized Self-Consistent Tight-Binding Quantum Chemical Method with Multipole Electrostatics and Density-Dependent Dispersion Contributions. *J. Chem. Theory Comput.* **2019,** *15* (3), 1652–1671.

(26) Neese, F. Software update: The ORCA program system-Version 5.0. *WIREs Comput. Mol. Sci.* **2022,** *12* (5), e1606.

(27) Lu, T.; Chen, Q. X. Shermo: A general code for calculating molecular thermochemistry properties. *Comput. Theor. Chem.* **2021,** *1200*, 113249.

(28) Zheng, X.; Li, Z.; Gao, W.; Meng, X.; Li, X.; Luk, L. Y. P.; Zhao, Y.; Tsai, Y.-H.; Wu, C. Condensation of 2-((alkylthio)(aryl)methylene)malononitrile with 1,2-aminothiol as a novel bioorthogonal reaction for site-specific protein modification and peptide cyclization. *J. Am. Chem. Soc.* **2020,** *142* (11), 5097–5103.

(29) Li, F.; Liu, J.; Liu, C.; Liu, Z.; Peng, X.; Huang, Y.; Chen, X.; Sun, X.; Wang, S.; Chen, W.; Xiong, D.; Diao, X.; Wang, S.; Zhuang, J.; Wu, C.; Wu, D. Cyclic peptides discriminate BCL-2 and its clinical mutants from BCL-XL by engaging a single-residue discrepancy. *Nat. Commun.* **2024,** *15*, 1476.

(30) Liu, J.; Sun, X.; Zhuang, J.; Liu, Z.; Xu, C.; Wu, D.; Wu, C. Biphenyl-dihydrothiazole-cyclized peptide libraries for peptide ligand and drug discovery. *Sci. China Chem.* **2025,** *68*, 1434–1444.